White Rose Research Online

eprints@whiterose.ac.uk
https://eprints.whiterose.ac.uk
Universities of Leeds, Sheffield and York

Deposited via The University of York.

White Rose Research Online URL for this paper:
https://eprints.whiterose.ac.uk/id/eprint/180486/

Version: Published Version

**Article:**
Bradley, L. E., Streeter, M. J.V., Murphy, C. D. et al. (2021) Effect of laser temporal intensity skew on enhancing pair production in laser - Electron-beam collisions. New Journal of Physics. 095004. ISSN: 1367-2630

https://doi.org/10.1088/1367-2630/ac1ed6

**Reuse**
This article is distributed under the terms of the Creative Commons Attribution (CC BY) licence. This licence allows you to distribute, remix, tweak, and build upon the work, even commercially, as long as you credit the authors for the original work. More information and the full terms of the licence here: https://creativecommons.org/licenses/

**Takedown**
If you consider content in White Rose Research Online to be in breach of UK law, please notify us by emailing eprints@whiterose.ac.uk including the URL of the record and the reason for the withdrawal request.

UNIVERSITY OF LEEDS
University of Sheffield
UNIVERSITY of York

New Journal of Physics
The open access journal at the forefront of physics

Deutsche Physikalische Gesellschaft DPG IOP Institute of Physics

PAPER • OPEN ACCESS

# Effect of laser temporal intensity skew on enhancing pair production in laser—electron-beam collisions

To cite this article: L E Bradley *et al* 2021 *New J. Phys.* **23** 095004

View the article online for updates and enhancements.

You may also like

- What defines the quantum regime of the free-electron laser?
Peter Kling, Enno Giese, Rainer Endrich et al.
- Valid lower bound for all estimators in quantum parameter estimation
Jing Liu and Haidong Yuan
- Impact of the laser spatio-temporal shape on Breit–Wheeler pair production
A Mercuri-Baron, M Grech, F Niel et al.

This content was downloaded from IP address 213.31.72.128 on 16/11/2021 at 10:59

New Journal of Physics
The open access journal at the forefront of physics

Deutsche Physikalische Gesellschaft DPG
IOP Institute of Physics

Published in partnership with: Deutsche Physikalische Gesellschaft and the Institute of Physics

OPEN ACCESS

RECEIVED
30 May 2021

REVISED
5 August 2021

ACCEPTED FOR PUBLICATION
18 August 2021

PUBLISHED
9 September 2021

Original content from this work may be used under the terms of the Creative Commons Attribution 4.0 licence.

Any further distribution of this work must maintain attribution to the author(s) and the title of the work, journal citation and DOI.

PAPER

# Effect of laser temporal intensity skew on enhancing pair production in laser–electron-beam collisions

L E Bradley[1,2,*], M J V Streeter[3,4], C D Murphy[1], C Arran[1], T G Blackburn[5], M Galletti[2,6], S P D Mangles[3] and C P Ridgers[1]

[1] York Plasma Institute, Department of Physics, University of York, Heslington, York, YO10 5DD, United Kingdom
[2] Central Laser Facility, Rutherford Appleton Laboratory, Oxon, OX11 0QX, United Kingdom
[3] The John Adams Institute for Accelerator Science, Blackett Laboratory, Imperial College London, South Kensington, London SW7 2BZ, United Kingdom
[4] School of Mathematics and Physics, Queen's University Belfast, Belfast, United Kingdom
[5] Department of Physics, Chalmers University of Gothenburg, SE-41296 Gothenburg, Sweden
[6] GoLP Instituto de Plasmas e Fusão Nuclear, Instituto Superior Tecnico, Universidade de Lisboa, Av. Rovisco Pais 1049-001 Lisbon, Portugal
[*] Author to whom any correspondence should be addressed.

**E-mail:** laurence.bradley@stfc.ac.uk

**Keywords:** strong-field, quantum electrodynamics, radiation reaction, electron collisions, plasma optics, pair production

## Abstract

Recent high-intensity laser experiments (Cole *et al* 2018 *Phys. Rev. X* **8** 011020; Poder *et al* 2018 *Phys. Rev. X* **8** 031004) have shown evidence of strong radiation reaction in the quantum regime. Experimental evidence of quantum effects on radiation reaction and electron–positron pair cascades has, however, proven challenging to obtain and crucially depends on maximising the quantum parameter of the electron (defined as the ratio of the electric field it feels in its rest frame to the Schwinger field). The quantum parameter can be suppressed as the electrons lose energy by radiation reaction as they traverse the initial rise in the laser intensity. As a result the shape of the intensity temporal envelope becomes important in enhancing quantum radiation reaction effects and pair cascades. Here we show that a realistic laser pulse with a faster rise time on the leading edge, achieved by skewing the temporal envelope, results in curtailing of pair yields as the peak power is reduced. We find a reduction in pair yields by orders of magnitude in contrast to only small reductions reported previously in large-scale particle-in-cell code simulations (Hojbota *et al* 2018 *Plasma Phys. Control. Fusion* **60** 064004). Maximum pairs per electron are found in colliding 1.5 GeV electrons with a laser wakefield produced envelope $7.90 \times 10^{-2}$ followed by a short 50 fs Gaussian envelope, $1.90 \times 10^{-2}$, while it is reduced to $8.90 \times 10^{-5}$, a factor of 100, for an asymmetric envelope.

## 1. Introduction

Strong field quantum electrodynamics processes can be investigated with current high power petawatt (PW) lasers, reaching intensities $\sim 10^{21}$ W cm$^{-2}$. Two important processes are quantum radiation reaction (RR) and multiphoton Breit–Wheeler (BW) pair production. RR describes the self-force on a charged particle as it emits radiation. A classical description of this force is not sufficient in the interaction of energetic electrons with strong laser fields as the quantum parameter $\chi_e = |\mathbf{E}|_{RF}/E_{crit}$, which compares the ratio of the electric field in the rest frame of the electron $E_{RF}$ to the critical (Schwinger) field [4] $E_{crit} = 1.38 \times 10^{18}$ V m$^{-1}$ approaches unity. As $\chi_e$ approaches unity, 0.44 of the electron's energy is taken by the emitted photons [5, 6]. A complete quantum description of RR is impractical due to the large number of interactions the electrons undergo with the laser photons and instead a practical model has been developed [7–10]. These models require experimental validation with recent evidence showing signs of quantum effects on RR [1, 2]. These experiments used an all-optical setup where electrons were externally accelerated to >100 MeV and then collided with a counter-propagating laser pulse. The resulting Doppler

© 2021 The Author(s). Published by IOP Publishing Ltd on behalf of the Institute of Physics and Deutsche Physikalische Gesellschaft

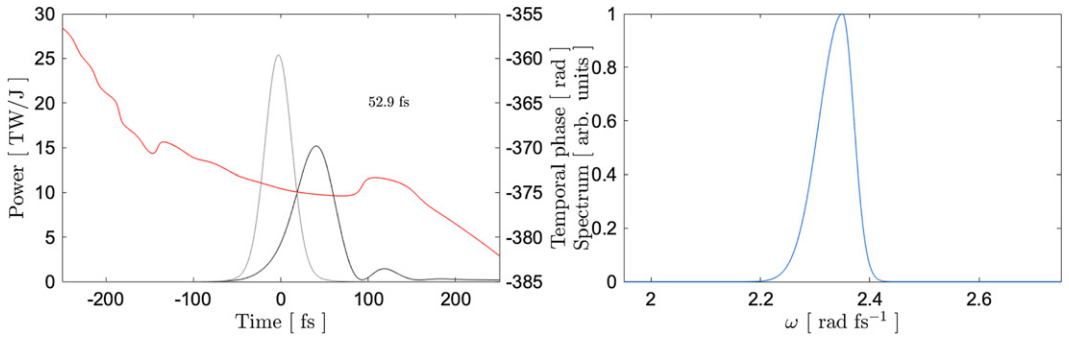


**Figure 1.** Example of a compressed Gaussian pulse before and after it is skewed. Shown in terms of power spectrum (black) and temporal phase (red) of the original and skewed envelopes (left) and the Fourier transformed spectrum (right).

upshift of the laser electric field results in $\chi_e \approx 0.02$–$0.2$. Similar experiments have been performed using crystals to provide the strong field [11].

Multiphoton BW pair production [12] occurs when a photon, emitted by an electron in the laser field, interacts with these fields and is converted to an electron-positron pair, $\gamma' + n\gamma \rightarrow e^+ + e^-$ [13]. This was observed at the SLAC facility using a moderate intensity of $I \sim 10^{18}$ W cm$^{-2}$ colliding with a 46.6 GeV beam (reached $\chi_e = 0.36$) [14]. However, at the moderate laser intensity the multiplicity of the interactions was not large and they may be described with a full QED calculation, which is not the case in current experiments at higher laser intensity.

As the electromagnetic fields produced with current PW laser systems are $E_L \sim 10^{-3} E_{crit}$, much lower electron energies are required to obtain the same $\chi_e$ as the SLAC experiment. Energies accessible to laser wakefield acceleration (LWFA $>$ 100 MeV) are sufficient and we may use an all-optical analogue to the SLAC experiment where a second laser pulse accelerates the electrons [15]. Recent electron energies from LWFA have been demonstrated at BELLA reaching a new record ∼7.8 GeV [16] although most LWFA experiments produce electron beams at ∼1 GeV so there is interest in how we may enhance the quantum parameter in all-optical collider experiments, for example employing an asymmetrical temporal envelope on the colliding pulse.

Modifying the laser pulse with a skew has been used in various simulations to show control of betatron oscillations [17] in a laser wakefield, enhanced proton acceleration [18] and increase electron–positron pair yields [3]. Most notably, in the Leemans experiments [19], it was shown that the asymmetry created by modifying the shape of a short 76 fs pulse improved electron yield in a plasma wakefield. Studies also report on the influence of a pulse asymmetry on the wake behaviour in LWFA simulations [20] and stability in the pointing angle of the electron-beam demonstrated experimentally [21].

Previous studies find enhancement in the yield of multi-photon BW pairs reported in simulations of an all-optical collider where the colliding pulse has a flat-top [22] and supergaussian temporal envelope [23]. In experiments, however, the finite bandwidth limitation of PW laser systems makes producing supergaussian temporal envelopes unattainable [24]. For enhancements to pair yields, this difference is associated to the electrons losing more or less energy to RR as they traverse the initial rise of the pulse [25]. There has not been an investigation of how temporal profiles which may be realistically produced and how the drop in peak power changes the pair yield. In this article we will perform such a study using the particle-in-cell (PIC) code EPOCH [26]. Our study uses parameters available with current PW laser systems with some results still relevant in experiments involving pair-plasma creation expected at multi-PW laser facilities [27, 28]. We will make comparison with BW pair production results from simulations in [3], in contrast using our realistic energy conserved laser intensity temporal envelopes. Pair production from colliding an electron bunch with a laser wakefield produced temporal envelope is also considered.

## 2. Modifying the laser temporal envelope using plasma optics

Control over the temporal envelope using traditional optics can be achieved using an acousto-optic programmable dispersive filter [29] (Dazzler) by changing the spectral phase of the pulse. Other examples of control using optical methods include changing the configuration of a pulse stretcher, shifting the grating distance of a chirp-pulse amplification compressor away from an optimal value or, produce high order phase components [30] in which a grating rotation gives a 3rd order phase component.

Plasma optics offers an attractive alternative to changing the laser temporal envelope. Experimental characterisation of pulses from a laser wakefield has been performed [31], relevant to above $a_0 = 1$, where

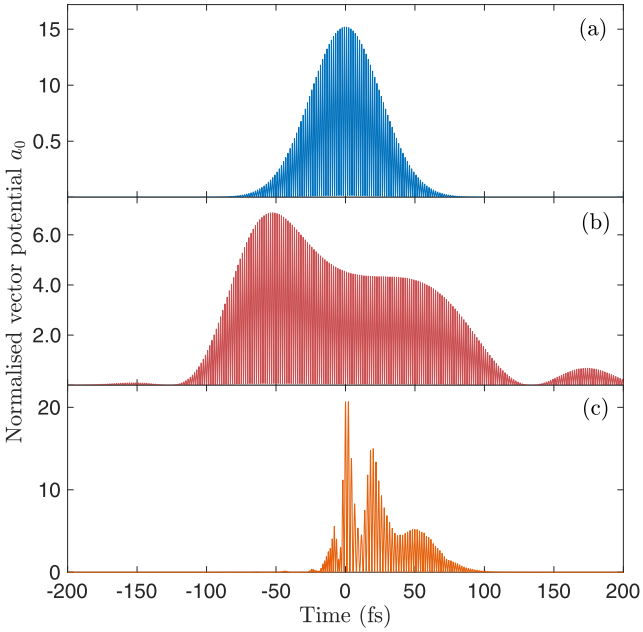


**Figure 2.** Simulating realistic laser temporal envelopes using a 50 fs symmetric Gaussian (blue), an asymmetric Gaussian generated by phase off-setting (red) and a pulse produced from a laser wakefield (orange). Simulation results on number of pairs per electron $N_{\pm}/N_e$ for the respective envelopes are provided in table 1.

**Table 1.** Simulating realistic pulse envelopes to determine pair yields for a 50 fs compressed Gaussian, a skewed temporal envelope and a pulse produced by an LWFA simulation in FBPIC code.

| Pulse shape | $a_0$ | $N_{\pm}/N_e$ |
|---|---|---|
| Symmetric 50 fs Gaussian | 15 | $1.90 \times 10^{-2}$ |
| Skewed temporal envelope | 7 | $8.90 \times 10^{-5}$ |
| Asymmetric LWFA envelope | 21 | $7.90 \times 10^{-2}$ |

asymmetric self-phase modulation has shown to shorten the pulse length with blueshift altering the rear and a redshift giving rise to steepening at the front of the pulse. Ellipsoidal plasma mirrors offer promising features by enhancing the laser contrast [32] and intensity [33] (expected increase $\sim 8$ at the PERL laser facility [34]), although with minimal effect on shaping the temporal envelope. One previous study has used plasma mirrors to study pair production enhancement [35] as well as other target and geometry parameters [36]. Two of the envelopes we simulate in our study can be produced using traditional optics via the methods aforementioned while the third envelope uses only plasma.

The first envelope is a short 50 fs optimally compressed Gaussian in (a) of figure 2. The skewed temporal envelope in (b) has been produced by a spectral phase off-setting and has a sharper rising edge and a slower trailing edge, in contrast to (c) which shows an envelope produced by driving the laser pulse through a 20 mm underdense plasma with electron density $n_e = 2 \times 10^{18}$ cm$^{-3}$. Figure 1 shows the peak reduction to the power spectrum by changing higher order phase components of a theoretical 53 fs Gaussian pulse. The plasma generated pulse has been produced with the Fourier–Bessel PIC (FBPIC) simulation code [37] and then simulated in our QED-PIC using EPOCH, described in section 4. Each of the three envelopes have been simulated respectively changing only the temporal envelope.

The envelopes in figure 2 are plotted in terms of the envelopes normalised vector potential $a_0$, where $a_0 \approx \sqrt{I\lambda_L^2/10^{18}\ \text{W cm}^{-2}\ \mu\text{m}^2}$, for a given laser intensity $I$ in units of W cm$^{-2}$ and wavelength $\lambda_L$ in microns. The magnitude of the peak $a_0$ is given in table 1 and differs considerably between the respective laser envelopes with the lowest $a_0$ for the skewed envelope. Another important distinction is that, although the LWFA generated pulse has the highest peak $a_0$, the pulse length is a lot shorter than the optimally compressed 50 fs Gaussian envelope or the longer skewed envelope. Electron bunches traversing these three envelopes will therefore experience different amounts of energy loss due to RR causing $\chi_e$ to change and the pair yields to be different in the three cases.

These envelopes were then simulated using the pair production QED-PIC code described in [7]. The electron–positron pair yields have been calculated, taking the ratio of the number of pairs $N_{\pm}$ to the total

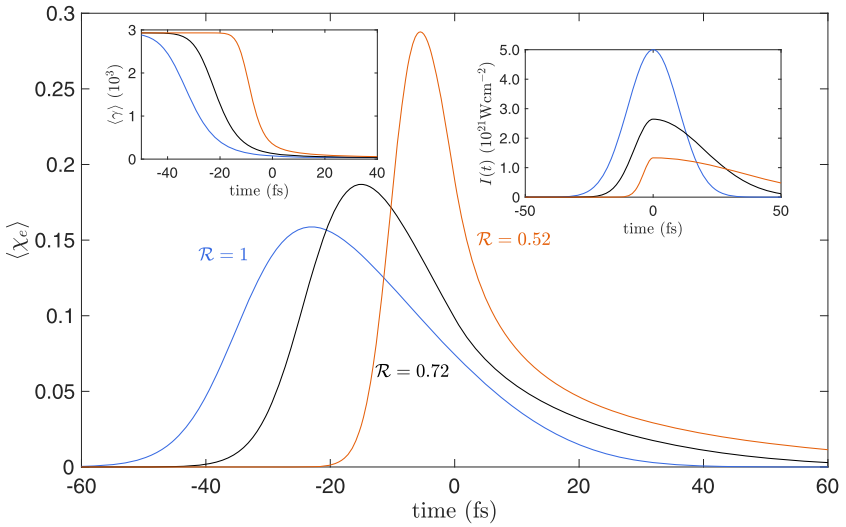


**Figure 3.** Average electron quantum parameter $\chi_e(t)$ for a Gaussian with different amounts of skew (right inset) using the closed form solution in equations (7) (left inset) and (8) with different reduction factors $\mathcal{R}$.

number of electrons in the electron bunch, after the collision with a 1.5 GeV ($\gamma_0 = 2931$) electron-beam. We calculate that the pair yields are maximum after interaction with the laser wakefield generated pulse, where $N_\pm/N_e = 7.90 \times 10^{-2}$, followed by the short 50 fs compressed Gaussian $N_\pm/N_e = 1.90 \times 10^{-2}$ and giving lowest pairs is the skewed envelope with $\sim 10^2$ magnitude lower, $N_\pm/N_e = 8.90 \times 10^{-5}$. This drop found to the number of pairs produced per electron are consistent with the following results, as we go on to describe the effect of skewing the temporal envelope of theoretical Gaussian laser pulses.

## 3. Analytical solution for a simplified asymmetric temporal envelope

Consider the temporal envelope to be Gaussian and written as the piecewise defined spectrum

$$I(t) = \begin{cases} I_0 \exp(-t^2/\tau_r^2) & \tau_r < t_0 \\ I_0 \exp(-t^2/\tau_f^2) & \tau_f > t_0, \end{cases} \tag{1}$$

where the peak intensity is related to the electric field by $I_0 = 0.5 c \epsilon_0 E_0^2$ and $E_0$ is the associated peak electric field. Modified envelopes may be produced by varying the two parameters $\tau_r$ or $\tau_f$ corresponding to the rise and fall times respectively. A symmetric Gaussian is recovered by setting $\tau_r = \tau_f$. The total pulse duration $\tau_p$ (FWHM) is then related to the rise and fall times by $\tau_p = 0.5(\tau_r + \tau_f)$. In order to keep the energy in the pulse constant we multiply the peak intensity of the skewed pulse relative to that of an unskewed Gaussian with e-folding time $\tau_0$ by $2\tau_0/\tau_p$. In order to keep the skewed pulse energy conserved we also derive the reduction factor $\mathcal{R}$ used to scale the intensity envelope, (full derivation in appendix A.1)

$$\mathcal{R} = \frac{2\tau_p}{\tau_r + \tau_f}. \tag{2}$$

The skewed pulse in figure 1 and the inset of figure 3 gives indication of the affect pulse skewing has on the peak temporal intensity in our simulations. This is important as it ensures equal comparison so that the pulse energy is always conserved (identical energy to the Gaussian pulse) by lowering the peak intensity of the skewed envelope. We also impose a condition in the choice of values for the rise $\tau_r$ and fall times $\tau_f$ such that $2\tau_p < \tau_r + \tau_f$ as this is the case for energy conservation to be satisfied, so $\mathcal{R} < 1$ and $I_1 < I_0$. Consider the case, pertinent to the all-optical collider, of a relativistic electron-beam counter-propagating relative to a skewed laser pulse. Assume the electron-beam is monoenergetic with initial energy $\mathcal{E}_0 = \gamma_0 m_e c^2$. If the hard photon (energies $E_\gamma \sim$ MeV) emission from these electrons is synchrotron-like (valid for $I_0 \gg 10^{18}$ W cm$^{-2}$), the energy evolves according to

$$m_e c^2 \frac{\mathrm{d}}{\mathrm{d}t}\langle\gamma\rangle = -\mathcal{P}(\chi_e), \tag{3}$$

where $\langle\gamma\rangle$ is the average electron Lorentz factor and $\mathcal{P}(\chi_e)$ is the instantaneous radiated power [38]

$$\mathcal{P}(\chi_e) = \frac{2}{3}\frac{\alpha_f c}{\lambda\!\!\!^{-}_c} m_e c^2 \chi_e^2 g(\chi_e), \tag{4}$$

where $\alpha_f \approx 0.0073$ is the fine structure constant and $\lambda\!\!\!^{-} \approx 3.86 \times 10^{-13}$ m is the reduced Compton wavelength. Here the Gaunt factor $g(\chi_e)$ [39] accounts for the reduction in the emitted power and is a correction to the synchrotron emission spectrum, due to quantum effects [40]. An approximate fit to this function is given by (full definition in appendix A.2)

$$g(\chi_e) = [1 + 4.8(1+\chi_e)\ln(1+1.7\chi_e) + 2.44\chi_e^2]^{-2/3}. \tag{5}$$

Since the electrons propagate counter to the laser pulse, $\chi_e \approx \gamma/E_{\text{crit}}|\mathbf{E}_\perp + \mathbf{v}\times\mathbf{B}|$ ($\mathbf{E}_\perp$ is the electric field perpendicular to the electron's motion) is

$$\chi_e = 2\gamma(t)\frac{E_L(t)}{E_{\text{crit}}}, \tag{6}$$

where the laser electric field temporal envelope has the form

$$E_L(t) = E_0\ \exp(-t^2/2\tau_p^2).$$

Note a conversion factor is introduced here in the definition of $E_L(t)$ from the relation $I \propto E^2$. Now we determine the solution of equation (3) for the asymmetric temporal envelope by substituting equation (6) into the instantaneous power radiated (4) and solving the differential equation in (3) to find the average behaviour of $\gamma$

$$\langle\gamma(t)\rangle = \begin{cases} \gamma_0/\left(1+\delta(1+\text{erf}(t/\tau_r)\right) & \tau_r < t_0 \\ \gamma_0/\left(1+\delta(1+\text{erf}(t/\tau_f)\right) & \tau_f > t_0, \end{cases} \tag{7}$$

where the term $\delta = 2\sqrt{\pi}\tau_{r,f}\gamma_0\alpha_f c E_0^2/(3\lambda_c E_{\text{crit}}^2)$ which depends on the peak laser electric field $E_0$, duration $\tau_{r,f} = 0.5\tau_p$ and initial Lorentz factor $\gamma_0$. We can now simply derive the classical average quantum parameter of the electrons by multiplying (7) by the relation of $\chi_e$ in (6) to find

$$\langle\chi_e(t)\mathcal{R}\rangle = \begin{cases} \chi_0\xi^{-1}\mathcal{R}\ \exp(-t^2/2\tau_r^2) & \tau_r < t_0 \\ \chi_0\xi^{-1}\mathcal{R}\ \exp(-t^2/2\tau_f^2) & \tau_f > t_0, \end{cases} \tag{8}$$

where $\chi_0$ is the initial quantum parameter before entering the pulse and we define the term $\xi = 1+\delta(1+\text{erf}(t/\tau_{r,f}))$. The validity of this equation agrees with equation (7) found in [41] which has been solved as a function of the phase $\chi_e(\phi)$. Taking the derivative of the average $\chi_e$ gives the time at which the average electron $\chi_e(t)$ is maximised in the envelope (i.e. when $\mathrm{d}\langle\chi_e(t)\rangle/\mathrm{d}t = 0$)

$$\frac{\mathrm{d}}{\mathrm{d}t}\langle\chi_e(t)\rangle = \frac{\chi_0 t}{\xi\tau_p^2}\ \exp(-t^2/2\tau_{r,f}^2) + \frac{\chi_0\gamma_0}{\xi^2\tau_R}\ \exp(-3t^2/2\tau_{r,f}^2), \tag{9}$$

where

$$\tau_R = \frac{3}{8}\frac{\lambda\!\!\!^{-}_c}{\alpha_f c}\left(\frac{E_{\text{crit}}}{E_0}\right)^2.$$

These equations describe a classical RR on the electrons and does not account for quantum effects. A modified-classical model in which equation (8) includes $g(\chi_e)$ to give $\langle\chi_e(t)g(\chi_e)\rangle$ has been solved numerically and is plotted in figure 3 simulated with three increasing amounts of skew controlled by the rise time $\tau_r$. Here we have shown two important observations; the first is that the electrons rate of energy loss is less than with the skewed envelope and therefore changing the shape of the synchrotron emission spectra, verified by PIC simulation in figure 7. Secondly, the time in which the average $\chi_e$ is maximised is extended in the Gaussian case and slowly decreases whereas the peak $\chi_e$ is shorter and decreases much more rapidly for the asymmetric envelope. We find peak $\langle\chi_e\rangle \approx 0.15$ in colliding a Gaussian pulse and a factor 2 increase $\langle\chi_e\rangle \approx 0.3$ if the envelope has a significant skew while the intensity is scaled by 0.52.

## 4. Simulating asymmetric temporal envelopes in a QED-PIC code

EPOCH PIC code was used to simulate the collision of the laser pulse with the electron-beam. The photon emission is calculated in the QED-PIC by using a Monte Carlo algorithm [7] capturing quantum stochasticity in the emission and resulting RR. These assumptions use the weak field ($E_L \leqslant 10^{-3}E_{\text{crit}}$) and

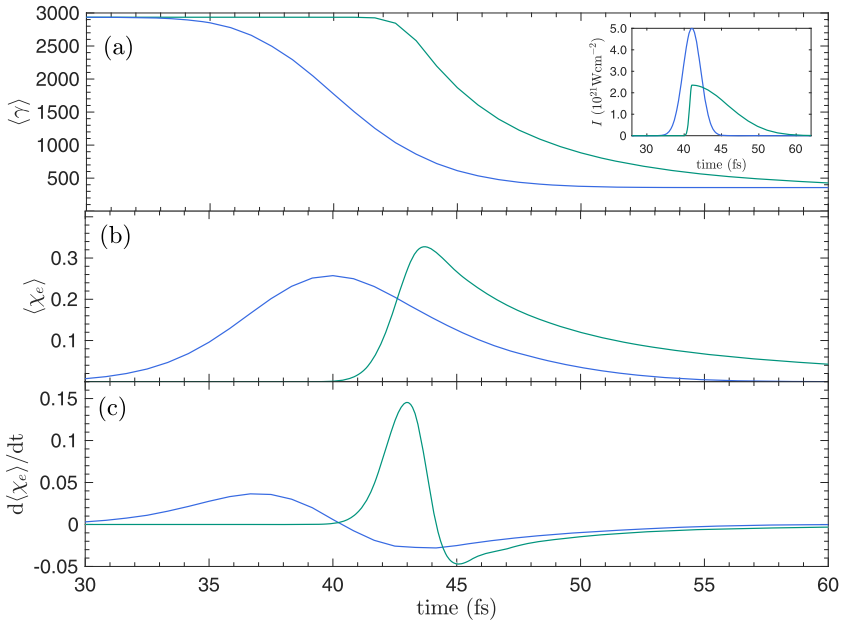


**Figure 4.** PIC code simulation showing the average behaviour of the 1.5 GeV electrons as they collide with the laser pulse and immediately lose energy to RR. (a) Average Lorentz factor $\langle\gamma\rangle$, (b) average quantum parameter $\langle\chi_e\rangle$ and (c) the derivative of $\langle\chi_e\rangle$. (Inset) Showing $I_0$ of the blue optimally compressed Gaussian envelope ($\mathcal{R} = 1$) and a negatively skewed Gaussian with peak $I_1$ ($\mathcal{R} < 1$) in green.

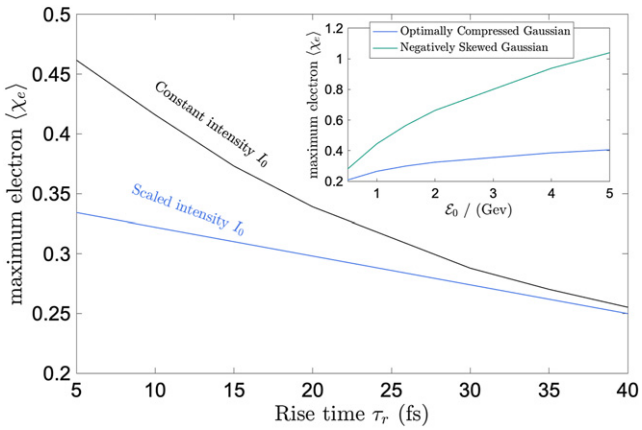


**Figure 5.** Maximum average electron $\chi_e$ as a function of the rise time $\tau_r$ as the front of a Gaussian pulse is skewed. Assuming a constant unchanged intensity spectrum $I_0$ (black) and with a decreasing $I_0$ such that $I_1 = \mathcal{R}I_0$ (blue). (Inset) Maximum average electron $\chi_e$ as a function of initial electron-beam energy $\mathcal{E}_0$ from 500 MeV up to 5 GeV.

the quasi-static approximations. This is to ensure that the formation length of the emitted hard photons are smaller than the laser wavelength so that the emission can be treated as synchrotron-like. In simulating BW pair production, we use a pair creation multiplier, multiplying the rate by a large factor and then dividing the weight of the produced pairs by the same fraction.

Our investigation uses the following simulation parameters. A domain which is $-100\ \mu\mathrm{m} \leqslant x \leqslant 100\ \mu\mathrm{m}$ with $10^3$ global grid points. The laser enters the simulation box from the left-hand boundary and has a 1 micron wavelength, $5 \times 10^{21}$ W cm$^{-2}$ peak intensity and is circularly polarised with a pulse duration (FWHM) of $\tau_\mathrm{p} = 40$ fs. The electron bunch, propagating from the right-hand boundary, consists of $10^5$ macroparticles. Convergence tests have been performed on the number of pairs produced per electron as a function of both macroparticles to represent the bunch and convergence on the simulation grid points. These tests were performed in order to determine that our baseline parameters have converged on the number of pairs produced. The electron-beam is monoenergetic with an initial beam energy centred at 1.5 GeV and initial density $n_\mathrm{e} = 1.8 \times 10^{18}$ m$^{-3}$. The electrons travel in the $-x$ direction (initial position at $x_0 = 99\ \mu$m) colliding with the laser pulse at time $t$.

**Table 2.** Results from four simulation runs with a Gaussian and skewed Gaussian laser envelope giving the maximum quantum parameter and number of electron–positron pairs produced per electron at the end of the collision.

| Simulation | $I_{0,1}(10^{21}$ W cm$^{-2})$ | $\mathcal{E}_0$ | max$\langle\chi_e\rangle$ | $N_\pm/N_e(10^{-6})$ |
|---|---|---|---|---|
| 1 | 5 | 1.5 | 0.255 | 19.60 |
| 2 | 3.7 | 1.5 | 0.272 | 6.20 |
| 3 | 2.9 | 1.5 | 0.291 | 2.80 |
| 4 | 2.4 | 1.5 | 0.313 | 1.50 |

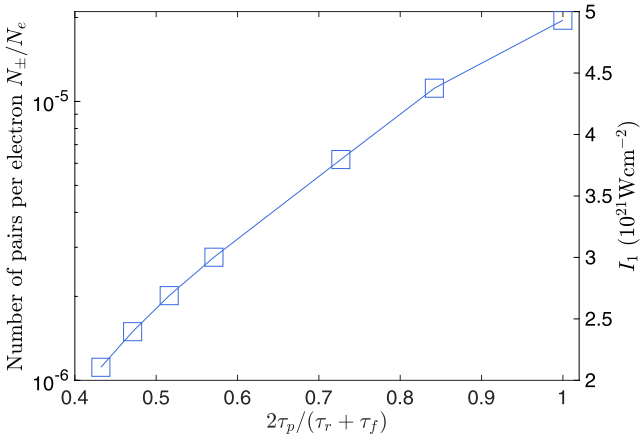


**Figure 6.** PIC code results showing the electron–positron pair yields per electron $N_\pm/N_e$ as the laser envelope is skewed. As the rising edge of a $I_0 = 5 \times 10^{21}$ W cm$^{-2}$ Gaussian laser pulse becomes faster, the peak intensity drops by a factor $\mathcal{R}$ giving the new peak intensity $I_1 = \mathcal{R}I_0$, displayed on the right-hand axis.

### 4.1. Skew effect on maximising the electron quantum parameter

Measuring the energy spread of the electron energy distribution after the interaction with the laser provides a clear indication of which RR model is observed [42, 43]. In a real RR experiment, both the electron energy spread as well as the photon energy spectra is measured. Our main focus is on the influence that skew has to the electron quantum parameter and how it is enhanced to maximise $\chi_e$. This parameter depends on the collision angle [44], the initial electron beam energy and the shape of the laser envelope. Here we only consider the latter as we assume the electrons are counter-propagating relative to the laser pulse (i.e. the collision is head-on). By changing the laser pulse duration and amount of asymmetry in the pulse, we may determine the effect that a skewed laser envelope has on maximising the bunches peak $\langle\chi_e\rangle$. These results are shown in figure 4 giving the average Lorentz factor in (a), average quantum parameter in (b) and its derivative in (c). Observe that as $\langle\chi_e\rangle$ for the skewed envelope is maximum for the interaction in (b), the Gaussian pulse gives a peak $\langle\chi_e\rangle$ over a longer interaction time $\sim$ 3fs. In (c) where the derivative passes zero, we can see the temporal displacement of peak $\chi_e$ in which the Gaussian pulse has a maximum $\langle\chi_e\rangle \approx 0.25$ at around $\approx$ 40 fs while this is slightly later for the negatively skewed envelope at $\approx$ 44 fs, where peak $\langle\chi_e\rangle > 0.3$.

Figure 5 shows the maximum electron average $\chi_e$ as a function of the rise time for both a constant Gaussian intensity along with a scaled intensity $I_1 = \mathcal{R}I_0$. This linear dependence found on the rise time of the intensity envelope in this figure is expected in a non-deterministic emission model as the photon spectrum becomes hardened [45]. The rapid increase of the black line shows that with the omission of $\mathcal{R}$ in equation (1), the increase in $\langle\chi_e\rangle$ is almost double as the rise time, becoming considerably shorter as the pulse is further skewed. This resulting difference is because of the competition between peak intensity and the time in which the electrons pass through the envelope and experience energy loss by RR. In the case of the Gaussian envelope, the electron bunch could have already produced high-energy photons. These PIC code results, while agreeing with the analytical result of figure 3, shows the model predicts that the initial energy of the electron bunch is critical in maximising the electron's $\chi_e$ and secondly that shorter pulses encourage maximum average $\chi_e$ because of the shorter interaction time as the electrons pass through the laser envelope. Therefore, the time in which $\chi_e$ is maximum in the pulse is some time before reaching the most intense part of the pulse, namely at the peak intensity $I_0$. This shows a skew on the colliding envelope is therefore beneficial in reaching maximum peak $\langle\chi_e\rangle$.

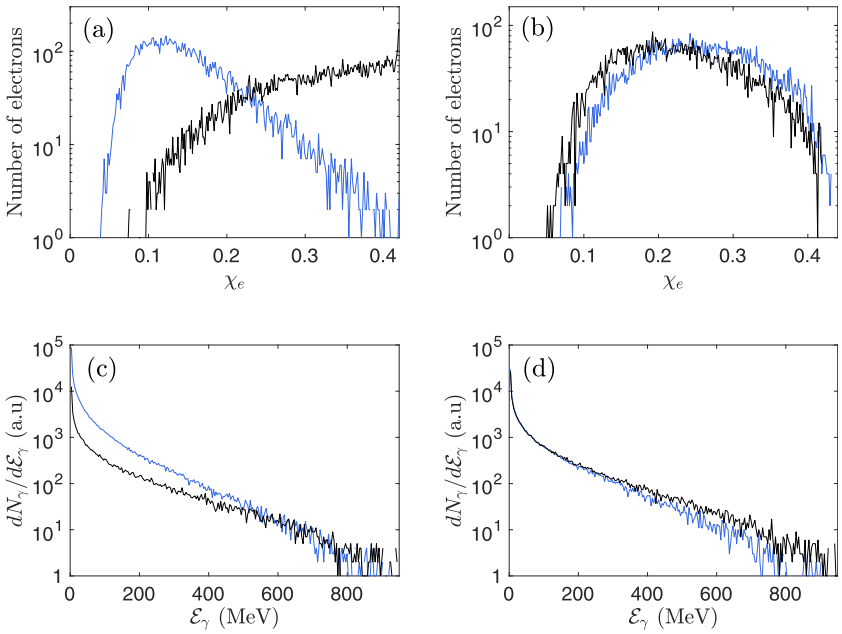


**Figure 7.** Comparing the change to the distribution in the electron quantum parameter $\chi_e$ and photon energy spectrums as the electrons are located at the peak intensity (a)–(c) and 8 fs (b)–(d) after a Gaussian (blue) and skewed Gaussian (black) pulse collides with a 1.5 GeV electron-beam.

### 4.2. Effect that the temporal envelope has on electron-positron pair yields

We are now in a position to determine the effect that skewing the envelope has on electron–positron pair yields. Four simulations have been ran with varying degree of skew to the envelope, giving the number of pairs per electron $N_\pm/N_e$ provided in table 2. Furthering our results alongside the results for realistic envelopes in section 2, we have considered the pair yields via the BW process recording the pair yields as skew is added, by decreasing the rise time in the range 5 fs $\leqslant \tau_r \leqslant$ 40 fs to resolve a Gaussian while the intensity is accordingly scaled ($\mathcal{R} < 1$). This result is shown in figure 6, finding that as the peak temporal intensity drops from optimal $5 \times 10^{21}$ W cm$^{-2}$ down to $2.4 \times 10^{21}$ W cm$^{-2}$, the pair yield is reduced by an order of magnitude. We find pairs per electron for a short 40 fs optimally compressed envelope is $1.96 \times 10^{-5}$, while with the extreme skewed envelope, pair yields are reduced to $1.50 \times 10^{-6}$. These simulations are also used to see the effect skew has in the electron $\chi_e$ distribution and photon energy spectrum for this corresponding number of pairs per electron.

These are provided in figure 7 once the electrons are at the peak of the Gaussian and skewed Gaussian envelopes (a) and (c). Also plotted are the distributions at some later time (8 fs) after the electron bunch is at the peak of the pulse in (b) and (d). RR has clearly changed the electron $\chi_e$ distribution for the Gaussian envelope where $\langle\chi_e\rangle$ is lower, while finding that the skewed envelope has more electrons with a significantly higher average $\chi_e$. In fact, at the peak of the pulse, the average electron $\chi_e$ for the skewed Gaussian is 0.23 and with the optimally compressed Gaussian is 0.16. At 8 fs after the peak, these averages are 0.23 and 0.22 respectively. This difference becomes less clear after the peak of the pulse with both skewed or unskewed distributions converging. This behaviour is also identified in the photon energy spectrums $\mathrm{d}N_\gamma/\mathrm{d}\mathcal{E}_\gamma$ which shows that at the peak there is a shape distinction between the soft lower energy photons, suggesting greater energy loss with the Gaussian pulse. This also becomes less observable in comparison after the electrons have traversed beyond the peak of the pulse. Finally, simulations in a higher intensity regime with parameters relevant to multi-PW laser facilities were performed. The reduction to the number of pairs for the skewed envelope in this regime is now the same order as with the Gaussian pulse. A 5.0 GeV electron bunch with a maximum quantum parameter of $\chi_e \approx 9$, produced electron–positron pairs per electron of $N_\pm/N_e = 0.19$ after colliding with a 40 fs Gaussian $I_0 = 1 \times 10^{23}$ W cm$^{-2}$ peak intensity laser pulse and $N_\pm/N_e = 0.11$ with the comparable skewed envelope.

## 5. Discussion

This simulation study has attempted to show the effect that the laser intensity temporal envelope has on enhancing electron–positron pair yields in a variety of envelope cases. The maximum pairs per electron

found in section 2 for the pulse generated in an LWFA scenario shows that a plasma-based method, employing skew with plasma optics, gives enhanced pair production via BW and is the ideal method. Further investigation may consider how different plasma densities influence the laser envelope to control the rise and fall times and find parameters that give the maximum intensity $a_0^2$ over short durations. In section 3, we gave equations describing the average Lorentz factor $\gamma$ and considered how the average electron $\chi_e$ evolves in time in the laser envelope for symmetric and asymmetric pulses. In consistency with simulation results in [46], these results show that the pulse duration and initial energy of the electron-beam is critical to maximising $\chi_e$ throughout the interaction and therefore presenting the most significant change to the synchrotron emission spectrum.

The results of our study have been made in contrast to the pair production yields in figure 3 of [3]. In figure 3(a) nonlinear BW pairs are shown to decrease for $S = -0.7$ but increase by a small factor for a skew of $S = 0.7$ ($S = 0$ is no skew). We show in figure 6 that BW pairs decrease by an order of magnitude from $2 \times 10^{-5}$ to $1.5 \times 10^{-6}$ pairs per electron once a significant skew is applied to the envelope, namely $\tau_r = 10$ fs and $\tau_f = 160$ fs. This is because in our simulation methodology, a combination of maximum peak intensity and a fast rising leading edge at the front of the pulse is unattainable in a realistic laser pulse. As a result of ignoring energy conservation, the laser intensity spectrum of skewed pulses as in [3], when compressed are unphysical with a sharp peak power.

Figure 5 shows the importance of keeping the energy in the skewed and non-skewed envelopes constant. Ignoring this and omitting the scaling by $\mathcal{R} = 2\tau_p/(\tau_r + \tau_f)$ to the peak intensity while skewing the envelope presents unphysical results in which the average $\chi_e$ is overestimated and appears high. We have also shown similar effects occurring in figure 5 (inset) as the initial electron beam energy increases, a skewed envelope gives a maximum $\langle \chi_e \rangle$ of 1.0 while it is only 0.4 for the optimally compressed Gaussian pulse. This suggests that while $\chi_e$ is maximised by a temporal skew, this is at the detriment of producing higher energy photons over longer times that may go on to produce pairs.

This naturally leads to consider the effect that electron straggling [47] has on the electrons in an envelope with a faster rise time. As a result of the probabilistic nature of the quantum emission process for $\chi_e \geqslant 0.1$, some electrons may reach the peak of the temporal envelope without emitting any or very few high-energy photons. If one finds straggling in a sufficient number of electrons, it would be beneficial in that electrons would reach the pulse peak with high values of $\chi_e$, as the rate of energy loss of these electrons is lower and significant energy remains for possible pair production [48], reports that straggling increases the number of pairs and that a lower intensity can be compensated by straggling electrons. In realistic RR experiments as the laser is focused, the electrons experience varying intensities along longitudinal slices of the bunch, as reported in the Gemini RR experiment [1]. Therefore, in theory a pulse with a faster rising leading edge could improve the number of straggling electrons as they reach the peak of the pulse on a shorter time duration. This effect can be seen in figure 4(b) in the PIC simulations, where straggling is taken into account, the electrons have a higher maximum average $\chi_e$ after traversing the skewed envelope.

As we mainly focus on showers of electron–positron pairs at lower values of $\chi_e \sim 0.3$ and not avalanches in which further pairs are produced after the initial pair creation [49]. It was necessary to consider our results more broadly in a higher intensity regime. Figure 1 in [6] shows the scaling of $\chi_e$ as a function of laser intensity. Here it is noted that at intensities $> 10^{23}$ W cm$^{-2}$, the quantum parameter begins to saturate and therefore so does the total number of pairs. Therefore, in this intensity regime, a reduction to peak intensity may not change the final pair yields substantially and so the Gaussian and skewed Gaussian collisions would generate similar numbers of pairs. At the end of section 4.2, simulations were ran to determine whether the reduced pairs seen in figure 6 for the skewed envelope still holds for $\chi_\gamma > 1$. Equal orders of magnitude in pair yields for both Gaussian and skewed Gaussian pulses were obtained. This suggests that above an intensity threshold, the order of magnitude increase to pair yields with the optimally compressed pulse is lost.

Employing a skew to the laser temporal envelope and changing the peak field strength changes the pair production probability rate [50]. In the trident pair production process, in which an electron produces a pair in a strong field via a virtual photon, the production rate depends on the electron energy and strength of the field. For BW pairs, this creation is by real photons interacting with the external field and depends more on the shape of the synchrotron emission spectrum. A change in the shape of the spectrum of figure 7 can be seen at the peak of the pulse and explains the higher number of pairs for a short 40 fs compressed pulse. Further investigation could compare these two pair production processes as was studied in [3], not ignoring the trident pair production process as we have in this study. This has been ignored due to the complex PIC modelling of this process and overall validity concerns of QED processes in PIC codes [51–54].

## 6. Conclusion

In conclusion, we have shown that skewing the laser intensity temporal envelope, lowering the peak intensity, gives a lower electron–positron pair yield per electron $1.5 \times 10^{-6}$ compared to optimally compressed $1.9 \times 10^{-2}$, or in colliding an electron-beam with a pulse generated using plasma optics $7.9 \times 10^{-2}$. We have considered how the electron quantum parameter $\chi_e$ evolves in a pulse with a temporal skew, showing $\chi_e$ is maximised not at the most intense part of the pulse but some time before significant energy loss to RR. While the electrons that reach the peak in a shorter interaction time of a skewed envelope have a higher maximum average $\chi_e$, this advantage is compensated by a lower pair yield as the energy in the laser is conserved by reducing the peak intensity as expected with current PW class laser systems. Our results provide evidence that colliding electrons into a laser envelope with a skew at the front of the pulse yields lower BW pairs, leading to enhanced pair production at current or future multi-PW facilities with either a short optimally compressed Gaussian or pulses generated by driving a laser wakefield.

## Acknowledgments

Computing resources were provided by STFC Scientific Computing Department's SCARF cluster.

## Data availability statement

The data that support the findings of this study are openly available at the following URL/DOI: https://etheses.whiterose.ac.uk/25601/1/Bradley_thesis.pdf.

### A.1. Conserving the energy in an asymmetric temporal envelope

Let the total energy in an optimally compressed Gaussian pulse be

$$\mathcal{E}_C = \int_{-\infty}^{\infty} I_0 \, \exp(-(t/\tau_p)^2)\mathrm{d}t = I_0 \tau_p \sqrt{\pi} \tag{10}$$

given the relation that

$$\int_{-\infty}^{\infty} \exp(-x^2)\mathrm{d}x = \sqrt{\pi}. \tag{11}$$

Consider splitting the integrals for the asymmetric envelope as follows

$$\begin{aligned}\mathcal{E}_S &= \int_{-\infty}^{0} I_1 \, \exp(-(t/\tau_r)^2)\mathrm{d}t + \int_{0}^{\infty} I_1 \, \exp(-(t/\tau_f)^2)\mathrm{d}t \\ &= \left(\int_{-\infty}^{0} I_1 \, \exp(-(t/\tau_r)^2)\mathrm{d}t + \int_{0}^{\infty} I_1 \, \exp\left(-\,(t/\tau_f)^2\,\mathrm{d}t\right)\right) \\ &= \frac{1}{2}\sqrt{\pi} I_1 (\tau_r + \tau_f).\end{aligned} \tag{12}$$

By setting the energy in the compressed Gaussian equal to the energy in the asymmetric Gaussian, we may find the ratio of intensities

$$I_0 \tau_p \sqrt{\pi} = \frac{1}{2}\sqrt{\pi} I_1 (\tau_r + \tau_f).$$

Solving for $\mathcal{R}$ factor

$$\mathcal{R} = \frac{I_1}{I_0} = \frac{2\tau_p}{(\tau_r + \tau_f)}. \tag{13}$$

### A.2. Quantum synchrotron emissivity

The Gaunt factor $g(\chi_e)$ (figure 8) is responsible for modifying the photon spectrum leading to a reduction to the radiated power in equation (4). It is given by integrating the photon synchrotron function

$$g(\chi_e) = \frac{\int_0^{\chi_e/2} F(\chi_e, \chi_\gamma)\mathrm{d}\chi_\gamma}{\int_0^{\infty} F_c\left(\frac{4\chi_\gamma}{3\chi_e^2}\right)\mathrm{d}\chi_\gamma} = \frac{3\sqrt{3}}{2\pi\chi_e^2}\int_0^{\chi_e/2} F(\chi_e, \chi_\gamma)\mathrm{d}\chi_\gamma,$$

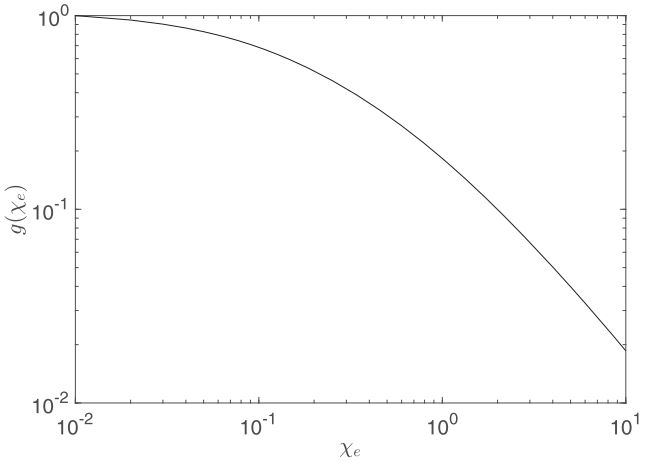


**Figure 8.** The approximate fit function of equation (5). A correction to the photon emission spectrum over a range of $\chi_e$ values for the semi-classical RR model. For classical RR $g(\chi_e)$ is unity.

where the function $F(\chi_e, \chi_\gamma)$ is the quantum synchrotron function provided by Sokolov and Ternov [55]

$$F(\chi_e, \chi_\gamma) = \frac{4\chi_\gamma^2}{\chi_e^2} y K_{2/3}(y) + \left(1 - \frac{2\chi_\gamma}{\chi_e}\right) y \int_y^\infty K_{5/3}(t)\mathrm{d}t,$$

where $y = 4\chi_\gamma/(3\chi_e(\chi_e - 2\chi_\gamma))$ and $K_n$ are modified Bessel functions of the second kind. In the classical limit as $g(\chi_e)$ is exactly unity, $F(\chi_e, \chi_\gamma)$ reduces to the classical synchrotron function $F_c(\chi_e, \chi_\gamma)$

$$F_c(\chi_e, \chi_\gamma) = y_c \int_{y_c}^\infty K_{5/3}(u)\mathrm{d}u,$$

where the term $y_c$ is $4\chi_\gamma/3\chi_e^2$ including $\chi_\gamma$ and $\chi_e$ which are the usual quantum parameters for the photon and electron respectively.

## ORCID iDs

L E Bradley https://orcid.org/0000-0001-7682-7221
M J V Streeter https://orcid.org/0000-0001-9086-9831
C D Murphy https://orcid.org/0000-0003-3849-3229
C Arran https://orcid.org/0000-0002-8644-8118
T G Blackburn https://orcid.org/0000-0002-3681-356X
M Galletti https://orcid.org/0000-0001-6928-0280
S P D Mangles https://orcid.org/0000-0003-2443-4201
C P Ridgers https://orcid.org/0000-0002-4078-0887

## References

[1] Cole J M *et al* 2018 Experimental evidence of radiation reaction in the collision of a high-intensity laser pulse with a laser-wakefield accelerated electron beam *Phys. Rev.* X **8** 011020
[2] Poder K *et al* 2018 Experimental signatures of the quantum nature of radiation reaction in the field of an ultraintense laser *Phys. Rev.* X **8** 031004
[3] Hojbota C I, Kim H T, Kim C M, Pathak V B and Nam C H 2018 Effect of the temporal laser pulse asymmetry on pair production processes during intense laser-electron scattering *Plasma Phys. Control. Fusion* **60** 064004
[4] Schwinger J 1951 On gauge invariance and vacuum polarization *Phys. Rev.* **82** 664–79
[5] Ridgers C P, Brady C S, Duclous R, Kirk J G, Bennett K, Arber T D, Robinson A P L and Bell A R 2012 Dense electron–positron plasmas and ultraintense $\gamma$ rays from laser-irradiated solids *Phys. Rev. Lett.* **108** 165006
[6] Bell A R and Kirk J G 2008 Possibility of prolific pair production with high-power lasers *Phys. Rev. Lett.* **101** 200403
[7] Ridgers C P, Kirk J G, Duclous R, Blackburn T G, Brady C S, Bennett K, Arber T D and Bell A R 2014 Modelling gamma-ray photon emission and pair production in high-intensity laser-matter interactions *J. Comput. Phys.* **260** 273–85
[8] Niel F, Riconda C, Amiranoff F, Lobet M, Derouillat J, Pérez F, Vinci T and Grech M 2018 From quantum to classical modeling of radiation reaction: a focus on the radiation spectrum *Plasma Phys. Control. Fusion* **60** 094002
[9] Sokolov I V, Naumova N M and Nees J A 2011 Numerical modeling of radiation-dominated and quantum-electrodynamically strong regimes of laser-plasma interaction *Phys. Plasmas* **18** 093109

[10] Vranic M, Martins J L, Fonseca R A and Silva L O 2016 Classical radiation reaction in particle-in-cell simulations *Comput. Phys. Commun.* **204** 141–51
[11] Wistisen T N, Di Piazza A, Knudsen H V and Uggerhøj U I 2018 Experimental evidence of quantum radiation reaction in aligned crystals *Nat. Commun.* **9** 795
[12] Breit G and Wheeler J A 1934 Collision of two light quanta *Phys. Rev.* **46** 1087–91
[13] Nikishov A I and Ritus V I 1964 Quantum processes in the field of a plane electromagnetic wave and in a constant field *Sov. Phys. JETP* **19** 529
[14] Bula C *et al* 1996 Observation of nonlinear effects in Compton scattering *Phys. Rev. Lett.* **76** 3116–9
[15] Thomas A G R, Ridgers C P, Bulanov S S, Griffin B J and Mangles S P D 2012 Strong radiation-damping effects in a gamma-ray source generated by the interaction of a high-intensity laser with a wakefield-accelerated electron beam *Phys. Rev.* X **2** 041004
[16] Gonsalves A J *et al* 2019 Petawatt laser guiding and electron beam acceleration to 8 Gev in a laser-heated capillary discharge waveguide *Phys. Rev. Lett.* **122** 084801
[17] Nam I, Hur M S, Uhm H S, Hafz N A M and Suk H 2011 Controlling the betatron oscillations of a wakefield-accelerated electron beam by temporally asymmetric laser pulses *Phys. Plasmas* **18** 043107
[18] Souri S, Amrollahi R and Sadighi-Bonabi R 2017 Laser-driven proton acceleration enhancement by the optimized intense short laser pulse shape *Phys. Plasmas* **24** 053108
[19] Leemans W P *et al* 2002 Electron-yield enhancement in a laser-wakefield accelerator driven by asymmetric laser pulses *Phys. Rev. Lett.* **89** 174802
[20] Zhang X *et al* 2012 Effect of pulse profile and chirp on a laser wakefield generation *Phys. Plasmas* **19** 053103
[21] Hafz N A M, Yu T J, Lee S K, Jeong T M, Sung J H and Lee J 2010 Controlling the pointing angle of a relativistic electron beam in a weakly-nonlinear laser wakefield accelerator *Appl. Phys. Express* **3** 076401
[22] Aleksandrov I A, Plunien G and Shabaev V M 2017 Pulse shape effects on the electron–positron pair production in strong laser fields *Phys. Rev.* D **95** 056013
[23] Abdukerim N, Li Z-L and Xie B-S 2013 Effects of laser pulse shape and carrier envelope phase on pair production *Phys. Lett.* B **726** 820–6
[24] Heritage J P, Weiner A M and Thurston R N 1985 Picosecond pulse shaping by spectral phase and amplitude manipulation *Opt. Lett.* **10** 609–11
[25] Ong J F, Moritaka T and Takabe H 2018 The suppression of radiation reaction and laser field depletion in laser-electron beam interaction *Phys. Plasmas* **25** 033113
[26] Arber T D *et al* 2015 Contemporary particle-in-cell approach to laser-plasma modelling *Plasma Phys. Control. Fusion* **57** 113001
[27] Myatt J, Delettrez J A, Maximov A V, Meyerhofer D D, Short R W, Stoeckl C and Storm M 2009 Optimizing electron–positron pair production on kilojoule-class high-intensity lasers for the purpose of pair-plasma creation *Phys. Rev.* E **79** 066409
[28] Lobet M, Davoine X, d'Humières E and Gremillet L 2017 Generation of high-energy electron–positron pairs in the collision of a laser-accelerated electron beam with a multipetawatt laser *Phys. Rev. Accel. Beams* **20** 043401
[29] Verluise F, Laude V, Cheng Z, Spielmann C and Tournois P 2000 Amplitude and phase control of ultrashort pulses by use of an acousto-optic programmable dispersive filter: pulse compression and shaping *Opt. Lett.* **25** 575–7
[30] Tóth C, Faure J, van Tilborg J, Geddes C G R, Schroeder C B, Esarey E and Leemans W P 2003 Tuning of laser pulse shapes in grating-based compressors for optimal electron acceleration in plasmas *Opt. Lett.* **28** 1823–5
[31] Schreiber J *et al* 2010 Complete temporal characterization of asymmetric pulse compression in a laser wakefield *Phys. Rev. Lett.* **105** 235003
[32] Rödel C, Heyer M, Behmke M, Kübel M, Jäckel O, Ziegler W, Ehrt D, Kaluza M C and Paulus G G 2011 High repetition rate plasma mirror for temporal contrast enhancement of terawatt femtosecond laser pulses by three orders of magnitude *Appl. Phys.* B **103** 295–302
[33] Wilson R *et al* 2016 Ellipsoidal plasma mirror focusing of high power laser pulses to ultra-high intensities *Phys. Plasmas* **23** 033106
[34] Kumar D *et al* 2019 Alignment of solid targets under extreme tight focus conditions generated by an ellipsoidal plasma mirror *Matter Radiat. Extremes* **4** 024402
[35] Gu Y-J, Klimo O, Bulanov S V and Weber S 2018 Brilliant gamma-ray beam and electron–positron pair production by enhanced attosecond pulses *Commun. Phys.* **1** 93
[36] Golub A, Villalba-Chávez S, Ruhl H and Müller C 2021 Linear Breit–Wheeler pair production by high-energy bremsstrahlung photons colliding with an intense x-ray laser pulse *Phys. Rev.* D **103** 016009
[37] Lehe R, Kirchen M, Andriyash I A, Godfrey B B and Vay J 2016 A spectral, quasi-cylindrical and dispersion-free particle-in-cell algorithm *Comput. Phys. Commun.* **203** 66–82
[38] Elkina N V, Fedotov A M, Kostyukov I Y, Legkov M V, Narozhny N B, Nerush E N and Ruhl H 2011 QED cascades induced by circularly polarized laser fields *Phys. Rev. Spec. Top. Accel. Beams* **14** 054401
[39] Gaunt J A and Fowler. R H 1930 Continuous absorption *Proc. R. Soc.* A **126** 654–60
[40] Andersen K K *et al* 2012 Experimental investigations of synchrotron radiation at the onset of the quantum regime *Phys. Rev.* D **86** 072001
[41] Blackburn T G, Ilderton A, Murphy C D and Marklund M 2017 Scaling laws for positron production in laser-electron-beam collisions *Phys. Rev.* A **96** 022128
[42] Ridgers C P *et al* 2017 Signatures of quantum effects on radiation reaction in laser-electron-beam collisions *J. Plasma Phys.* **83** 715830502
[43] Arran C, Cole J M, Gerstmayr E, Blackburn T G, Mangles S P D and Ridgers C P 2019 Optimal parameters for radiation reaction experiments *Plasma Phys. Control. Fusion* **61** 074009
[44] Blackburn T G, Ilderton A, Marklund M and Ridgers C P 2019 Reaching supercritical field strengths with intense lasers *New J. Phys.* **21** 053040
[45] Blackburn T G, Ridgers C P, Kirk J G and Bell A R 2014 Quantum radiation reaction in laser-electron-beam collisions *Phys. Rev. Lett.* **112** 015001
[46] Neitz N and Di Piazza A 2014 Electron-beam dynamics in a strong laser field including quantum radiation reaction *Phys. Rev.* A **90** 022102
[47] Shen C S and White D 1972 Energy straggling and radiation reaction for magnetic bremsstrahlung *Phys. Rev. Lett.* **28** 455–9
[48] Duclous R, Kirk J G and Bell A R 2010 Monte Carlo calculations of pair production in high-intensity laser-plasma interactions *Plasma Phys. Control. Fusion* **53** 015009

[49] Mironov A A, Narozhny N B and Fedotov A M 2014 Collapse and revival of electromagnetic cascades in focused intense laser pulses *Phys. Lett.* A **378** 3254–7
[50] Kirk J G, Bell A R and Arka I 2009 Pair production in counter-propagating laser beams *Plasma Phys. Control. Fusion* **51** 085008
[51] Blackburn T G, Seipt D, Bulanov S S and Marklund M 2018 Benchmarking semiclassical approaches to strong-field QED: nonlinear Compton scattering in intense laser pulses *Phys. Plasmas* **25** 083108
[52] Gonoskov A *et al* 2015 Extended particle-in-cell schemes for physics in ultrastrong laser fields: review and developments *Phys. Rev.* E **92** 023305
[53] Grismayer T, Vranic M, Fonseca R, Harvey C, Ilderton A, Marklund M and Oliveira Silva L 2012 On the path to pair production: self-consistent PIC modeling of high energy photons in laser-plasma interaction *APS Division of Plasma Physics Meeting Abstracts,* (*APS Meeting Abstracts* vol 54) p PP8.076
[54] Martinez B, Lobet M, Duclous R, d'Humières E and Gremillet L 2019 High-energy radiation and pair production by coulomb processes in particle-in-cell simulations *Phys. Plasmas* **26** 103109
[55] Sokolov A A and Ternov I M 1968 *Synchrotron Radiation* (Berlin: Akademie-Verlag)